J Fluoresc (2015) 25:729–738
DOI 10.1007/s10895-015-1559-4

ORIGINAL PAPER

Apparent Shear Sensitivity of Molecular Rotors in Various Solvents

Adnan Mustafic[1] · Kristyna M. Elbel[2] · Emannuel A. Theodorakis[2] · Mark Haidekker[1]

Received: 14 December 2014 / Accepted: 16 March 2015 / Published online: 29 March 2015

Abstract Fluorescent environment-sensitive dyes often change their spectral properties concomitantly with multiple solvent properties, such as polarity, protonation, hydrogen bond formation, or viscosity. Careful consideration of the response is needed when a fluorescent dye is used to report a single property. Recently, we observed an increase of emission intensity of viscosity-sensitive molecular rotors in fluids subject to flow and speculated that either polar-polar interaction or hydrogen bond formation play a role in the apparent flow sensitivity. In this study, we show experimental evidence that photoisomerization to an isomer with a lower quantum yield, first proposed by Rumble et al. (J Phys Chem A 116(44):10786–10792, 2012), plays a key role in the observed phenomenon. We subjected four molecular rotors with different electron acceptor motifs to fluid flow in solvents of different polarity and ability to form hydrogen bonds. We also measured the isomerization dynamics in a custom fluorophotometer with extremely low light exposure. Our results indicate that the photoisomerization rate depends both on the solvent and on the electron acceptor group, as does the recovery of the original isomer in the dark. In most solvents, recovery of the dark isomer is much more rapid than originally reported, and a state of quasi-equilibrium between both isomers is possible. Moreover, the sensitivity (i.e., relative intensity increase at the same flow rate) is also solvent-dependent. The intensity increase can be detected at very low velocities (as low as 0.06 mm/s). Characteristic for fluorescent dyes is the high spatial resolution, and no flow measurement device with comparable sensitivity and spatial resolution exists, although the nature of the solvent needs to be taken into account for quantitative flow measurement.

Keywords Molecular rotors · Flow sensors · Shear stress · Twisted intramolecular charge transfer states · TICT · Microfluidics · Photoisomerization

Mark A. Haidekker is Professor at the University of Georgia and holds a PhD degree in Computer Science from the University of Bremen, Germany

✉ Prof. Mark A. Haidekker
mhaidekk@uga.edu

[1] College of Engineering, University of Georgia, 597 D. W. Brooks Drive, Athens, GA 30602, USA

[2] Department of Chemistry & Biochemistry, University of California, San Diego, 9500 Gilman Drive MC: 0358, La Jolla, CA 92093-0358, USA

Introduction

Environment-sensitive fluorescent probes enjoy enormous popularity due to their ability to provide *in vivo* physiological information of cells or biological tissues on a microscopic level. Applications range from labeling proteins or DNA [1] to monitoring physiological processes, such as calcium channel activation, biomolecular interactions [2], or biophysical changes in the cell membrane [3]. Environment sensitivity predominantly depends on the interaction of a fluorophore dipole with its environment (e.g., solvatochromic shifts in environments of different polarity [4]), direct fluorophore-solvent interaction (e.g., quenching or hydrogen bond formation [5]), fluorophore-fluorophore interaction, and segmental mobility [6]. In fact, Lakowicz raises the concern that multiple simultaneous interactions create a complex spectral behavior that is difficult to attribute to one single environmental effect [1].

Characterizing of the interaction of a fluorophore with its environment is therefore subject of ongoing research, as is the development of new environment-sensitive probes with higher specificity towards one type of interaction.

Of particular interest are some dyes with segmental mobility that are capable of an intramolecular twisting motion in the excited state [6], which are often referred to as "molecular rotors" [7, 8]. Those molecules have two competing deexcitation pathways: (a) a pathway in which the molecule remains in a planar conformation when it returns to the ground state, and (b) a pathway in which the molecule assumes a twisted state before returning to the ground state. In the latter case, emission is either red-shifted [9] or completely nonradiative [10]. Simulations have shown that a representative molecular rotor, 9-(dicyanovinyl)-julolidine (DCVJ) has a preferred (i.e., lowest-energy) planar conformation in the ground state, whereas it assumes a lowest-energy twisted conformation at 90° in the excited state [11]. The reason for the nonradiative deexcitation lies in the low $S_1 - S_0$ energy gap in the twisted state.

Molecular rotors are known for their viscosity-dependent emission quantum yield [12]. Steric hindrance in high-viscosity solvents shifts the balance in favor of the planar, radiative deexcitation pathway, and a well-known empirical relationship between the viscosity η of the solvent and the molecular rotor's fluorescent quantum yield ϕ_F (Eq. 1) is known as the Förster-Hoffmann equation,

$$\phi_F = \phi_0 \cdot \left(\frac{\eta}{\sigma}\right)^x \tag{1}$$

where ϕ_0 is the dye's intrinsic quantum yield, σ is a dye-dependent constant with units of viscosity, and x is a dye- and solvent-dependent constant [13]. A more recent study gave rise to the notion that the power-law relationship described in Eq. 1 is caused by a combination of polar dye-solvent interaction and microviscosity-related steric hindrance [14]. Both the polarity of the solvent and its ability to form hydrogen bonds influence the twisted-state formation rate [15]. Consequently, both emission wavelength and quantum yield are influenced by multiple concomitant solvent properties that need to be taken into account when the fluorescence signal is interpreted. None the less, several studies demonstrate that the information provided by the fluorescence of molecular rotors is useful, and molecular rotors have been used, for example, to investigate protein conformal changes [16, 17], phopsholipid bilayer microviscosity [7], and the microviscosity of the interior of cells [18].

We reported an intriguing new phenomenon, whereby the fluorescence emission intensity increases in moving fluids [19]. This phenomenon can be seen in an experiment as simple as a stirred dye solution in a fluoroscopic cuvette. The intensity increase ΔI over the no-flow baseline was dependent both on the viscosity of the solvent η and the velocity of flow v, and ΔI could be described very accurately by the empirical relationship [19]

$$\Delta I = \Delta I_{max}\left(1 - \exp\left(-\frac{v}{v_0}\right)\right)\left(1 - \exp\left(-\frac{\eta}{\eta_0}\right)\right) \tag{2}$$

where ΔI_{max} is a solvent-dependent asymptotical intensity increase, and v_0 and η_0 are solvent-characteristic constants that govern the flow- and viscosity-dependency of the intensity increase. With a suitable experimental setup, the apparent flow sensitivity of molecular rotors allows to take images of flow patterns in microfluidic chambers [20]. Moreover, the sensitivity of the intensity increase at very low flow rates is unusually high, such that instruments of comparable sensitivity (e.g., heated-plate flow meters) show orders of magnitude lower spatial resolution, and flow measurement with comparable resolution (e.g., particle tracking) has much lower sensitivity.

Based on our studies, prerequisite for flow sensitivity is a polar functional group on the molecular rotor and a polar solvent: DCVJ (**1**) does not exhibit this phenomenon at all, and a carboxylic-acid derivative (CCVJ, **2**) does not exhibit this phenomenon in nonpolar fluids, such as hexanes [19, 20]. Based on these findings, we hypothesized that either polar-polar interaction or hydrogen bond formation play a role in the apparent flow sensitivity. Recently, a new explanation for this phenomenon was proposed by Rumble et al. [21], according to which molecular rotors with asymmetric headgroups (e.g., CCVJ, but not DCVJ) are capable of forming two distinct isomers: a fluorescent E-isomer and a nonfluorescent Z-isomer. According to this new hypothesis, E-Z isomerization is photoinduced and occurs on the time scale of a few seconds, whereas Z-E recovery in the dark takes several days. The apparent flow sensitivity in the cuvette experiment would be explained under this hypothesis as a consequence of new E-isomer that is introduced into the narrow excitation light beam when the fluid is stirred, while in the fluid at rest the rapid E-Z photoisomerization leads to a lower measured emission intensity [21].

To shed more light on the potential roles of photoisomerization processes and solvent polarity effects on the observed apparent flow sensitivity, we conducted a series of experiments with different molecular rotors in solvents of different polarity. The two research questions we tried to answer are (a) whether there is a possible relationship between flow rate, type of solvent and flow-induced observed intensity increase; and (b) under assumption of the E-Z isomerization hypothesis, whether there is a relationship between recovery time of the E-isomer and the type of solvent.

In this study, we used four molecular rotors shown in Fig. 1: 9-(2-carboxy-2-cyanovinyl)-julolidine) (CCVJ, **2**)

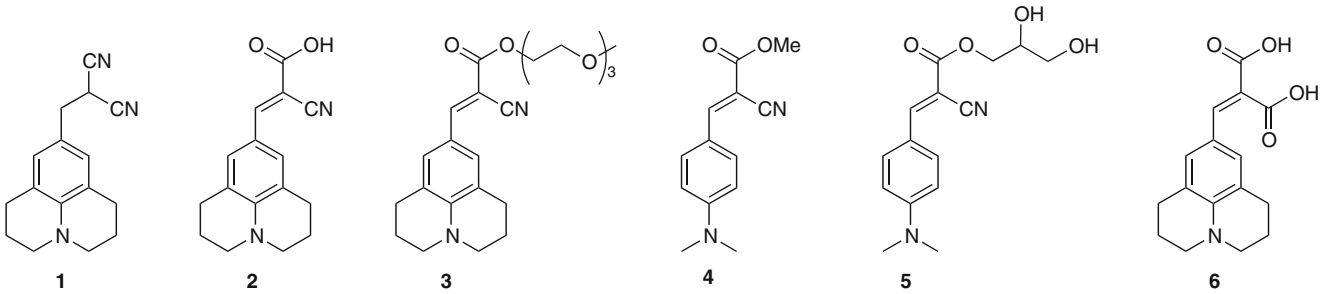

Fig. 1 Chemical structures of molecular rotors **1** (DCVJ, 9-(dicyanovinyl)-julolidine), **2** (CCVJ, 9-(2-carboxy-2-cyanovinyl)-julolidine), **3** (9-(2-carboxy-2-cyanovinyl)-julolidine) triethyleneglycol ester), **4** (p-[(2-cyano-2-methylester) vinyl] dimethylaniline), **5** (p-[(2-cyano-2-propanediol ester) vinyl] dimethylaniline), **6** (9-(dicarboxyvinyl)-julolidine). The axis of rotation is typically the 2-cyanoprop-2-enoic acid group with respect to the julolidine group (in the case of **1**, **2**, **3**, and **6**) and the aniline group (in the case of **4** and **5**) around which the molecules enter the twisted state

and an analog, 9-(2-carboxy-2-cyanovinyl)-julolidine) triethyleneglycol ester (**3**); p-[(2-cyano-2-methylester) vinyl] dimethylaniline (**4**) together with its more hydrophilic analog p-[(2-cyano-2-propanediol ester) vinyl] dimethylaniline (**5**). The choice of **3** was made to exclude the possibility that the carboxylic acid of **2** undergoes ester formation with the solvent. In addition, we examined 9-(dicarboxyvinyl)-julolidine (**6**) to differentiate between the influence of polar headgroups (such as the carboxyl group of **2**, which is absent in **1**) and the influence of a symmetrical headgroup that is unable to form isomers as in the case of **1**.

As solvents we used, in the order of increasing polarity, toluene, methanol, ethylene glycol, and dimethyl sulfoxide. All solutions were subjected to varying flow rates in a custom fluoroscopic quartz flow cuvette, and we report herein the flow- and solvent-dependent intensity increase of the different rotor-solvent combinations.

Materials and Methods

Molecular Rotors, Solvents, and Solution Preparation

CCVJ (**2**) was purchased from Sigma-Aldrich (St. Louis, MO). Compounds **3** − **6** were synthesized by our group as reported elsewhere [22]. The chemical structures are found in Fig. 1. Spectroscopy-grade methanol, ethylene glycol, toluene, and dimethyl sulfoxide (DMSO) were purchased from Sigma-Aldrich, and the relevant properties of these solvents are listed in Table 1. Stock solutions of all molecular rotors were prepared at a concentration of 5mM in DMSO. The stock solutions were kept at 4 °C until used. Solutions were prepared by pipetting 60 μL of the stock solution into 30 mL of the solvent under vigorous stirring for a resulting concentration of 10 μM.

Flow Apparatus and Flow Response Measurement

A square quartz tube with 4 mm outer side length (Technical Glass Products, Painesville Twp., OH) was placed between two sheets of aluminum that were in turn held in place by four steel posts (Thorlabs, Newton, NJ). The inlet of the quartz tube was connected to Teflon tubing (Restek Corp., Bellefonte, PA) via a two-way connector (Omnifit, Danbury, CT), which in turn was attached to a 30 mL glass syringe (Eisele Interchange, Nashville, TN). The outlet of the quartz tube was connected via a two-way connector to Teflon tubing, which in turn was attached to an empty, vertically mounted syringe cylinder to collect excess fluid that accumulates during solution pumping.

The quartz tube with its aluminum holding plates was placed inside the sample chamber of a fluorospectrometer (Fluoromax 3, Jobin-Yvon, Edison, NJ) and shielded from environmental light with blackout material (Thorlabs) with only the Teflon tubing protruding. The glass syringe was placed in a custom programmable syringe pump. Both the

Table 1 Some properties of solvents used in this study [23]

Solvent	Dipole Moment	Molecular Weight	Viscosity η mPa s (25 °C)	Dielectric Constant ε	Polarity
Ethylene glycol	2.36	62.068	16.06	41.40	Polar protic
Methanol	1.70	34.042	0.54	33.00	Polar protic
Dimethyl sulfoxide	3.96	78.133	2.47	48.90	Dipolar aprotic
Toluene	0.38	92.139	0.59	2.39	Non-polar

glass syringe and the collection syringe were exposed to regular room light during these experiments, but a background scan showed that environmental light did not raise the background photon counts inside the sample chamber.

The molecular rotor solutions (total of 12, with 3 molecular rotors and 4 solvents) were injected into the quartz tube at flow rates of 0.25, 0.50, 0.75, 1.00, 2.00, 3.00 and 4.00 ml/min, controlled by the syringe pump. All flow experiments were performed at room temperature of approximately 22 °C. The fluorophotometer recorded timecourse scans (i.e., intensity as a function of time) for each solution at the peak excitation and emission wavelengths. Three independent timecourse scans were acquired for each rotor/solvent combination. Before each flow rate was applied, a baseline was established for 300 seconds during which no solution was injected.

The absolute intensity increase ΔI for each flow phase was determined from the averaged intensity during the flow phase s and the baseline intensities b_1 and b_2 60 seconds before and after the flow according to Eq. 3:

$$\Delta I = s - \frac{b_1 + b_2}{2} \tag{3}$$

The procedure is illustrated in Fig. 2, which shows a section of a timecourse scan of a 10 μM solution of CCVJ in ethylene glycol at a flow rate of 0.50 ml/min.

Measurement of Z-E Recovery Dynamics

Following the hypothesis that E-Z isomerization is photoinduced and that Z-E recovery occurs in the dark over a period of many hours [21], we built a laser-induced fluorophotometer as follows: Up to four sample solutions (3.5 mL of each dye in glass cuvettes) were first irradiated by placing the samples in the collimated beam of a mercury arc lamp (Olympus) for 20 minutes to ensure complete conversion of the E-isomer to the Z-isomer. Immediately after light exposure, the samples were placed in a Turret-400 temperature-controlled sample holder (Quantum Northwest, Liberty Lake, WA). All samples were stirred continuously. A 440 nm, 4 mW laser (Crystalaser, Reno, NV) was used for excitation, and a ND10 filter (Thorlabs) was placed in its beam path to reduce the excitation intensity to 0.4 mW. A photomultiplier module (Hamamatsu H5784) together with a 480 ± 15 nm dichroic bandpass filter (Omega, Brattleboro, VT) were used along the perpendicular light path for emission collection. The assembly was encased in blackout material (Thorlabs). Under control of a custom controller, the Turret-400 was used to place one of the samples in the beam path, after which the laser was turned on for 65 ms and a reading acquired from the photomultiplier module. The laser was immediately turned off again, and the process repeated for the next sample. This measurement sequence was repeated once every 25 minutes. With an approximate FWHM beam diameter of 1.5 mm, the beam irradiates a volume of approximately 18 μL, which corresponds to 0.5 % of the total cuvette volume. With 65ms exposure every 25 minutes, the light-to-dark ratio was 43×10^{-6}. Even if saturation along the laser beam is assumed, the total cuvette light-to-dark ratio is 0.2×10^{-6}. The extreme light-to-dark ratio was necessary to ensure that Z-E recovery dominates over E-Z photoisomerization. During the entire duration of the measurement, temperature control of the Turret-400 was enabled, and a temperature of 22 °C was chosen. The controlled temperature was similar to room temperature, but the controller reduced potential temperature fluctuations in the laboratory environment.

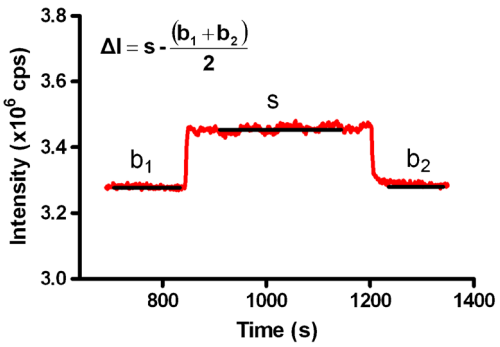

Fig. 2 A selected region of a timecourse scan of 10 μM CCVJ in ethylene glycol. Baseline intensities b_1 and b_2 are obtained from regions before and after a flow rate of 0.50 ml/min. The average intensity s during the flow phase was obtained, and the average baseline subtracted (Eq. 3) to obtain the absolute intensity increase ΔI

Statistical Analysis

Nonlinear regression was used to model the intensity increase ΔI as a function of flow rate v. Regression and further statistical analysis was performed with GraphPad Prism v.5 (GraphPad Software, Inc., La Jolla, CA). The model functions were the exponential association (Eq. 4), based on an earlier publication [19], and the Boltzmann sigmoidal (Eq. 5) that potentially better reflects low intensity increases in the low-flow region:

$$\Delta I = \Delta I_{max} \cdot \left(1 - e^{-\frac{v}{v_0}}\right) \tag{4}$$

$$\Delta I = \Delta I_{max} \cdot \frac{1}{1 + e^{\frac{v_{50} - v}{v_0}}} \tag{5}$$

In both equations, ΔI_{max} is the maximum intensity increase, v_0 the characteristic velocity, and v_{50} is the flow rate when the intensity increase is halfway between its smallest (in this case 0) and its largest value. All three model constants were obtained from the regression.

Since the absolute intensity depends on the viscosity of the solvent, we further examined a normalized intensity

increase, ΔI_{norm},

$$\Delta I_{norm}(v) = \frac{\Delta I(v)}{\Delta I_{max}} \quad (6)$$

under the assumption that the intensity increase is multiplicative. The two regression models were subjected to Akaike Information Criteria (AIC) to determine their goodness of fit and decide which model better represents the data.

Results

Representative timecourse scans of a 10 μM solution of CCVJ (**2**) in ethylene glycol are shown in Fig. 3 with flow rates increasing from 0.25 mL/min to 4 mL/min. Due to the limited volume of the syringe, a refill step was programmed between the 2 ml/min and 3 mL/min flow steps. The intensity change during the refill phase was not further used in the data analysis. Figure 3 shows excellent repeatability of the experiment during three independent repeats. Exceptions were found (a) with **6**, which showed no intensity increase with increased flow in any solvent, and (b) the combinations of **2** in DMSO and **5** in methanol, where no systematic intensity variation with flow could be found. One such inconsistent timecourse (**2** in DMSO) is shown in Fig. 4. These cases were excluded from further analysis.

Flow-Dependent Intensity Analysis

From the timecourse data of all dye/solvent combinations (with the exceptions listed above), eight data points of intensity increase over flow velocity were obtained, and nonlinear regression analysis provided the model constants

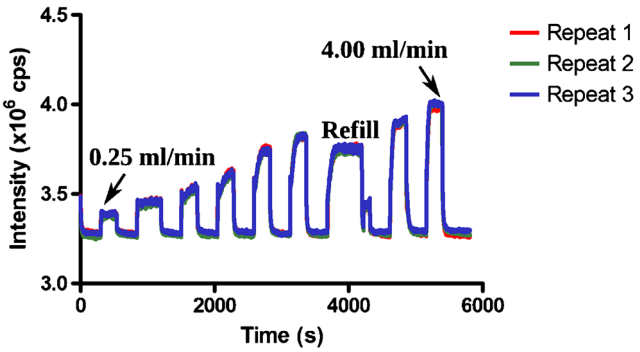

Fig. 3 Timecourse scans of a 10 μM solution of CCVJ in ethylene glycol ($N = 3$) with noticeable intensity increases during all periods of flow. It is evident that the intensity increase is not proportional to flow velocity at higher flow rates, which gives rise to the nonlinear regression models presented in Eqs. 4 and 5. The syringe was refilled between flow rates 2.00 mL/min and 3.00 mL/min as indicated in the figure, but the intensity plateau during the refill phase was discarded from further analysis

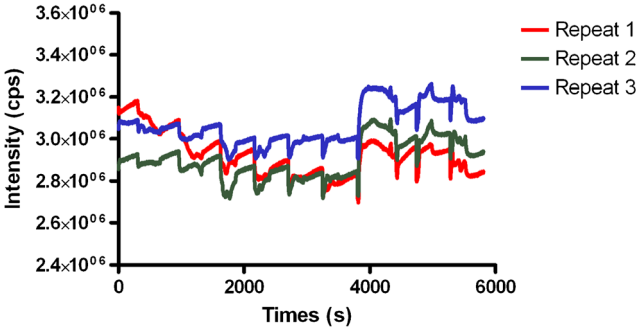

Fig. 4 Timecourse scan of a 10 μM solution of CCVJ in dimethyl sulfoxide where a relationship between increasing flow rates and increasing intensity during flow (as shown in Fig. 3) could not be established. The timecourse scans for the three repeats show a much larger variability than those seen in Fig. 3, and any baseline in the absence of flow could not be established

ΔI_{max}, v_0, and for the sigmoidal model, v_{50}. Based on the AIC analysis, the exponential association was the preferred model in eight cases (**2**, **3**, and **5** in ethylene glycol, **2** and **3** in methanol, **3** in Toluene and DMSO, and **5** in DMSO), while Boltzmann sigmoidal was the preferred model in only 2 cases (**2** and **5** in Toluene). Since the statistical model preferred in most cases was exponential association, we decided to use it for nonlinear regression in all data sets.

Nonlinear regression results are shown in Fig. 5, and the regression coefficients can be found in Table 2. In ethylene glycol, the values for ΔI_{max} were the highest for **3** (2293 cps), followed by **2** (1960 cps) and **5** (1457 cps). The characteristic flow rate v_0 was highest for **3** (2.88 mL/min), followed by **5** (2.16 mL/min) and **2** (1.8 mL/min). In methanol, results followed the same pattern with **3** having higher ΔI_{max} and v_0 (154 cps, 4.5 mL/min) than **2** (94.14 cps, 1.2 mL/min). In DMSO, **5** had higher values for ΔI_{max} (352.4 cps) than **3** (321.4 cps), while the values for v_0 were almost identical (1.003 mL/min vs. 1.005 mL/min). In toluene, a high ΔI_{max} for **2** (772×10^3 cps) and the low value for v_0 indicated a poor description of the data by the exponential model, mainly because the saturation effect seen in the other solvents is not as prominent in toluene. The normalized intensity ΔI_{norm} – the data points and regression results are shown in Fig. 6 – allows better comparison of the intensity increase across solvents of different viscosity. With the exception of toluene, the normalized intensity increase shows much less variability across the different dyes than the absolute intensity increase.

Z-E Isomer Recovery Dynamics

Compounds with symmetrical headgroups (**1**, **6**, and Lucifer Yellow, which was used as a control dye without molecular rotor characteristics) showed no change of intensity over time as measured with the custom laser fluorophotometer.

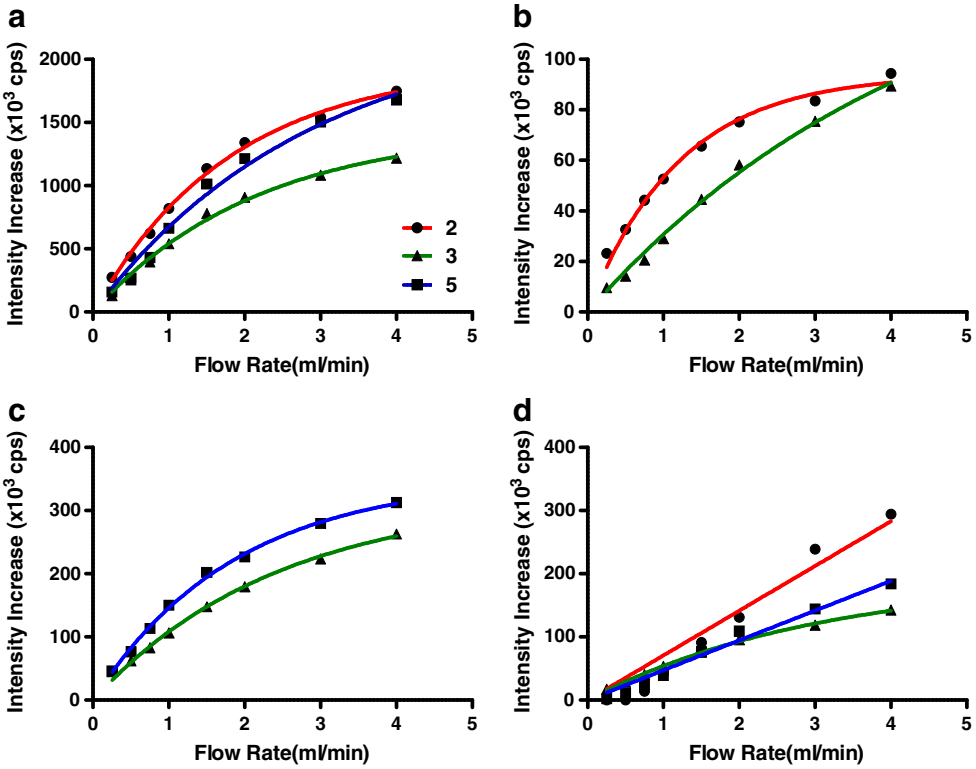

Fig. 5 Nonlinear regression of the absolute intensity increase over flow rate for molecular rotors **2**, **3**, and **5** in **A** ethylene glycol, **B** methanol, **C** dimethyl sulfoxide and **D** toluene

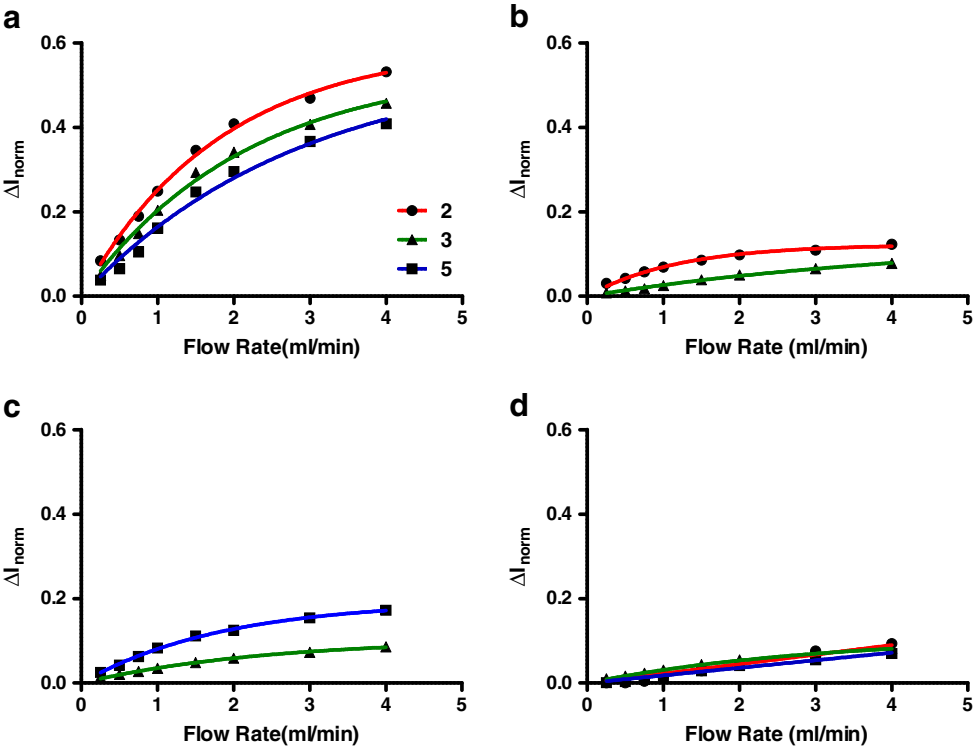

Fig. 6 Normalized exponential association curve fit of selected molecular rotors in **A** ethylene glycol, **B** methanol, **C** dimethyl sulfoxide and **D** toluene. ΔI_{norm} (given in %) is the flow-dependent intensity increase normalized by the baseline intensity

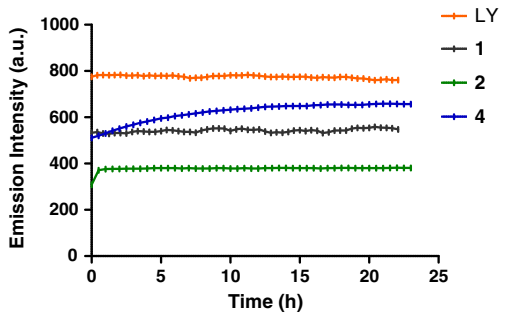

Fig. 7 Fluorescence intensity behavior, measured in the custom low-exposure laser fluorophotometer, of some dyes in ethylene glycol after exposure to strong white light. Intensity data are shown without any normalization. Shown are molecular rotors **1**, **2**, and **4** in ethylene glycol. For comparison, Lucifer Yellow (LY) is also shown. Intensity variation of DCVJ (**1**) shows no statistically significant correlation with time, and the intensity of Lucifer Yellow drops by about 0.7 %. Both **2** and **4** show exponential recovery dynamics with a time constant of 15 minutes and 6 hours, respectively. Note that Lucifer Yellow was diluted to approximately match the intensity of the molecular rotors

In addition, **6** showed no intensity variations in a cuvette with and without stirring [19] (data not shown). On the other hand, dyes with asymmetrical headgroup (**2**, **3**, and **4**) exhibited increasing intensity under the low exposure conditions of the custom laser fluorophotometer. Under the assumption of single-exponential photoisomerization and recovery dynamics, nonlinear regression was performed with Eq. 7,

$$I(t) = I_{Base} + I_E \cdot \left(1 - e^{-\frac{t}{T_E}}\right) \tag{7}$$

where I_{Base} is the baseline intensity at the start of the experiment after bright light exposure and considers unconverted E isomer and fluorescence of the Z isomer, I_E is the fluorescence contribution from recovered E isomer, and T_E is the Z-E recovery time constant. In most dye-solvent combinations, the recovery time constant was found in the order of less than one hour, and the time resolution of the custom instrument with one sample every 25 minutes did not allow accurate recovery of T_E from the data. For this reason, recovery data are given in a mostly qualitative fashion.

Figure 7 shows raw timecourse data of **1**, **2**, and **4**, and includes Lucifer Yellow (LY) as a control dye. Lucifer Yellow intensity dropped by 0.7 % over the observation period, and no significant correlation of the intensity of **1** with time was found. Conversely, the intensity dynamics of both **2** and **4** followed Eq. 7 with time constants T_E of approximately 15 minutes and 6 hours, respectively.

Due to its long recovery time constant, compound **4** provided a clear trend of increasing T_E with increasing polarity. We found values of T_E of 11 minutes in toluene, 1.9 hours in DMSO, and 3.6 hours in methanol. Somewhat similar trends of increasing T_E with increasing polarity were observed with the other dyes as well, but their much shorter recovery times introduced large errors into the best-fit values of T_E. In solvents of approximately similar polarity, but increasing viscosity (mixtures of ethylene glycol and glycerol with increasing glycerol content), CCVJ (**2**) showed decreasing time constants: 48 minutes in 32 mPa s, 18 minutes in 73 mPa s, 7 minutes in 165 mPa s, and 5 minutes in 374 mPa s (Fig. 8). Recovery time constants T_E were less consistent with dye **5**, although they also showed a trend to shorter recovery times with 49 minutes (32 mPa s), 24 minutes (73 mPa s), 27 minutes (165 mPa s), and 22 minutes (374 mPa s). Once again, short recovery times push the resolution limit of the instrument, and some recovery may have taken place during the transfer of the samples from the light exposure site to the custom fluorometer as evidenced by the higher relative intensity at the start of the experiment.

Discussion

In a previous study, we reported a novel environment-sensitive behavior of molecular rotors [19] whereby an increased emission intensity is observed in molecular rotor solutions under flow. In the present study, we aimed to validate the E-Z isomerization hypothesis, and to find a possible

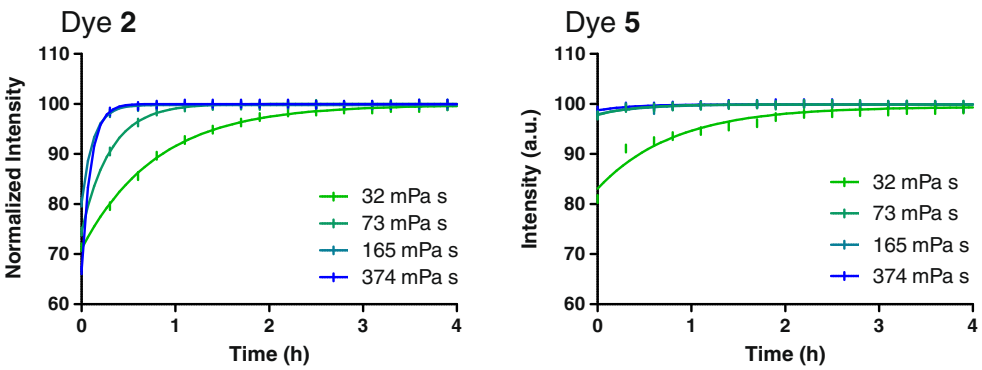

Fig. 8 Fluorescence intensity recovery of **2** and **5** in mixtures of ethylene glycol and glycerol of different viscosities. A general trend can be observed that higher viscosities lead to shorter E-isomer recovery times. Intensity values have been normalized to reach 100 % at $t \to \infty$, and the curve shows the best-fit curve from Eq. 7

relationship between flow rate, type of solvent and flow-induced observed intensity increase. Our original working hypothesis for the flow-sensitive behavior was either hydrogen bond formation or polar-polar interaction between dye and solvent [19], mostly based on the observation that DCJV (**1**) did not show any apparent flow sensitivity, and that none of the dyes showed this effect in nonpolar solvents (i.e., hexanes). An alternative hypothesis, formulated by Rumble et al. stipulated the existence of a photoinduced Z-isomer of low quantum yield. Isomerization requires the presence of an asymmetric headgroup, and the isomerization hypothesis is predominantly favored by our observation that the symmetric compound **6** does not show the apparent flow effect and behaves similarly to DCVJ, although it has a polar headgroup. Moreover, the E-Z photoisomerization hypothesis helps explain two observations that are otherwise difficult to interpret, that is, (a) a slow decay after cessation of flow and (b) the apparent saturation at high flow rates (see, e.g., Fig. 3). When the solvent is at rest, the excitation light causes isomerization to the Z isomer. Conversely, when the solvent flows past the excitation beam, fresh E isomer is introduced into the light path, and the observed intensity increases.

We observed a relatively slow decay of the intensity to baseline after cessation of flow, which would be explained by the formation of the Z isomer over several seconds of illumination of the stagnant solvent. The decay constant is in the range of 3.5 to 4.5 seconds (see the falling intensity edge in Fig. 3) and therefore much lower than the time constant of 7.5 minutes given by Rumble et al. [21]. The flow apparatus used in this study is incapable of measuring the time constant of Z isomer formation, because elasticity of the tubing causes a small amount of flow to continue even after the syringe pump stopped. In fact, we found that using shorter and more rigid tubing as well as a glass syringe reduced the intensity decay time [19]. The decay time would best be measured in a stagnant, dark-adapted solution (E isomer) where an intensity timecourse is recorded immediately after the sample is exposed to excitation light. Due to the low variability of the decay times (i.e., the Z isomer formation rate), we did not pursue this question further.

We also observed an apparent saturation at high flow rates (as described by ΔI_{max} in Eq. 2), where a further increase of the intensity is not possible even at much higher flow rates. This observation can be explained by the upper limit of unexposed E-isomer that is pushed into the excitation beam by flow. In this case, the velocity of the fluid is fast enough that no significant Z isomer formation takes place. Flow velocities in the quartz tube range from 0.06 mm/s to almost 1 mm/s. At the lowest flow rate, a fluid particle needs about 16 seconds to traverse the beam, and at the highest flow rate, 1 second. The latter time is much lower

Table 2 Regression coefficients obtained from the exponential curve fit of data

Solvent	Coefficient	**2**	**3**	**5**
Ethylene glycol	ΔI_{max}	1960	1457	2293
	ΔI_{norm}	0.596	0.558	0.547
	v_0	1.826	2.156	2.877
	R^2	0.996	0.993	0.986
Methanol	ΔI_{max}	94.14	154	*
	ΔI_{norm}	0.123	0.133	*
	v_0	1.201	4.500	*
	R^2	0.987	0.995	*
DMSO	ΔI_{max}	*	321.4	352.4
	ΔI_{norm}	*	0.105	0.195
	v_0	*	1.005	1.003
	R^2	*	0.995	0.998
Toluene	ΔI_{max}	772376	193.6	14314
	ΔI_{norm}	245	0.111	5.44
	v_0	1.09×10^{-6}	3.045	333.33
	R^2	0.942	0.998	0.976

*represents the exceptional cases, such as the one shown in Fig. 4, where a relationship between flow and intensity could not be established

than the Z-isomerization time constant given by Rumble et al. as 7.5 minutes [21] and still lower than the time constants of 3.5 to 4.5 seconds found in this study. At high flow rates, therefore, the solvent traverses the excitation beam before significant amounts of Z isomer can be formed, and the intensity saturates at the intensity level of pure E isomer. The flow rate is inversely proportional to the persistence time of the solvent in the excitation beam, and an argument can be made that the time constant v_0 in Table 2 is inversely related to the Z isomer formation rate.

The results of this study provide experimental evidence that photoinduced isomerization to a state with reduced quantum yield takes place. However, this study also shows the fundamental role played by the solvent. We showed that the interaction of the molecular rotor with its solvent plays a significant role in the recovery in the dark of the higher-quantum yield E-isomer (Figs. 7 and 8). We also showed that the flow-dependent intensity increase depends on the solvent used (Table 2). The photoisomerization hypothesis stipulates that the intensity increase is caused by the introduction of E isomer into the beam. Therefore, we conclude that either the photoisomerization rate is highly solvent-dependent or additional effects, such as the influence of polarity, play an additional role. In fact, we now interpret the apparent flow sensitivity as a combination of viscosity-dependent, but flow-independent intensity increase, combined with photoisomerization in the presence of strong excitation light.

The first conclusion from this study, therefore, is that the solvent strongly influences the isomerization dynamics. We found that increased polarity increased the recovery time constant (and thus slowed down the E isomer recovery rate). Interestingly, an increased viscosity, created with a higher glycerol content in an ethylene glycol-glycerol mix, decreased the recovery time. Although viscosity creates a microfriction barrier for the formation of twisted states, in a cautious interpretation, isomer formation appears not to be hindered by viscosity.

The second conclusion from this study is that recovery of the E isomer in the dark is much faster than anticipated [21]. Experiments in the low-exposure laser fluorophotometer confirm the short time constant. In addition, the short recovery time constant is necessary to explain why we were able to see flow-dependent intensity in the first place: Since we refilled the syringe with already-exposed dye solution (from the flow phases at 0.25 mL/min to 2 mL/min), the intensity increase after the refill (at 3 mL/min and 4 mL/min) should have been markedly lower than before the refill step. In fact, since the glass syringe was exposed to room light throughout the experiment and experiment setup, there should arguably not have been any intensity increase at all. However, with recovery times in the order of minutes, the persistence time inside the tubing (and thus in the dark) gives us enough E isomer to see the flow-dependent intensity change.

The relatively slow traversal of the excitation beam by the solvent in combination with a relatively short recovery time of the E isomer gives rise to the notion of a state of quasi-equilibrium. The normalized intensity ΔI_{norm} is highest in ethylene glycol (Fig. 6), i.e., the solvent with the highest viscosity. The normalization removes the higher baseline intensity that is directly caused in high-viscosity solvents by reducing the twisted-state formation rate (Eq. 1). Our observation from the low-exposure fluorophotometer that solvents with high viscosity reduce the recovery time of the E isomer allow us to interpret the result as an increased availability of E isomer at the point of measurement.

Compounds **3** and **5** showed a clear flow-dependent intensity increase in DMSO. Although the normalized intensity increase is much lower than the one observed in ethylene glycol, it is not very different from methanol. Since DMSO is an aprotic solvent, hydrogen bond formation does not appear to influence the isomerization process. Notably different from the other solvents is the behavior in toluene, where the data points of both absolute and relative intensity increase over flow are much smaller than in DMSO or methanol (Fig. 5). First, toluene is a low-viscosity solvent. In combination with its low polarity, Z-E recovery can be fast enough to allow a state of quasi-equilibrium, whereby only small amounts of excess E isomer exist in the dark, and small amounts of excess Z isomer in the excitation beam, causing the observed low intensity change with flow.

Moreover, the asymptotic intensity increase of ΔI_{norm} gives an indication of the relative fluorescence difference between the E- and Z-isomers. A larger value indicates a larger difference in quantum yield between the two isomers. With values of ΔI_{norm} that range from approximately 0.1 to 0.6 (the toluene data, which fit the model poorly, set aside), the Z isomer has between 90 % and 40 % of the quantum yield of the E isomer. The most striking difference is between ethylene glycol and all other solvents. Since ΔI_{norm} is based on viscosity-corrected intensities, we can speculate that the Z isomer has a lower viscosity sensitivity (i.e., a lower value for x in Eq. 1) than the E isomer.

Lastly, the functional group of the molecular rotor itself influences the flow-sensitive effect. As seen in Fig. 6, CCVJ (**2**) has a consistently higher intensity increase than the other two molecular rotors, and **5** shows the lowest intensity increase. It could be speculated that the intensity increase follows the reactivity of the functional group, which would indicate that the recovery rate of the E isomer is reduced when the molecule has a more reactive head group.

Our experiments were designed with the purpose of discerning additional information about molecular rotors which can help us with the understanding of their physical

interaction with solvent molecules. We hypothesized that one of the underlying causes of shear sensitivity of molecular rotors is their ability to form hydrogen bonds. This was proved not to be the case. However, experiments in different solvents give an indication that the solvent's viscosity and polarity as well as the molecular rotor's functional group are involved in the intensity response to flow. We have found additional evidence that the recently discovered formation of a photoisomer [21] plays an important role in the flow response, but E-Z isomerization alone cannot explain all observations. Moreover, the isomer formation and recovery dynamics are in themselves strongly solvent-dependent. With this additional knowledge, molecular rotors of the class examined herein may reveal even more information about the solvent than previously known.

In conclusion, the observed effect of increased emission intensity following increased flow rate in microfluidic systems gives rise to a highly sensitive flow sensor with spatial resolution limited only by the limits of the optical system. Images of the intensity increase are strikingly similar to computed fluid dynamics simulations [20], but those images reveal minute irregularities of the flow system that would not normally be considered in computational fluid dynamics. Such a flow sensor has many potential applications in fluid dynamics studies, microfluidics, mixing problems, and closed-loop flow control.

References

1. Lakowicz JR (2006) Solvent and environmental effects. In: Lakowicz JR (ed) Principles of fluorescence spectroscopy. Springer, Berlin Heidelberg New York, pp 205–235
2. Klymchenko AS, Mély Y (2012) Fluorescent environment-sensitive dyes as reporters of biomolecular interactions. In: Morris MC (ed) Fluorescence-based biosensors: from concepts to applications. Academic Press, London, pp 35–58
3. Demchenko AP, Mély Y, Duportail G, Klymchenko AS (2009) Monitoring biophysical properties of lipid membranes by environment-sensitive fluorescent probes. Biophys J 96(9):3461–3470
4. Von Lippert EZ (1957) Spektroskopische Bestimmung des Dipolmomentes aromatischer Verbindungen im ersten angeregten Singulettzustand [Spectroscopic determination of the dipole moment of aromatic compounds in the first excited singlet state]. Zeitschrift für Elektrochemie, Berichte der Bunsengesellschaft für physikalische Chemie 61(8):962–975
5. Von Lippert EZ (1957) Der Einfluss von Wasserstoffbrücken auf Elektronenspektren [The influence of hydrogen bonds on electronic spectra]. In: Hadzi D (ed) Hydrogen Bonding. Pergamon Press, New York, pp 217–257
6. Grabowski ZR, Rotkiewicz K, Rettig W et al (2003) Structural changes accompanying intramolecular electron transfer: focus on twisted intramolecular charge-transfer states and structures. Chem Rev–Columbus 103(10):3899–4032
7. Kung CE, Reed JK (1986) Microviscosity measurements of phospholipid bilayers using fluorescent dyes that undergo torsional relaxation. Biochemistry 25(20):6114–6121
8. Iwaki T, Torigoe C, Noji M, Nakanishi M (1993) Antibodies for fluorescent molecular rotors. Biochemistry 32(29):7589–7592
9. Grabowski ZR, Rotkiewicz K, Siemiarczuk A, Cowley DJ, Baumann W (1979) Twisted intramolecular charge transfer states (TICT). A new class of excited states with a full charge separation. Nouveau J Chim 3(7):443–453
10. Chang TL, Cheung HC (1990) A model for molecules with twisted intramolecular charge transfer characteristics: solvent polarity effect on the nonradiative rates of dyes in a series of water—ethanol mixed solvents. Chem Phys Lett 173:343–348
11. Allen BD, Benniston AC, Harriman A, Rostron SA, Yu C (2005) The photophysical properties of a julolidene-based molecular rotor. Phys Chem Chem Phys 7(16):3035–3040
12. Abdel-Mottaleb MSA, Loutfy RO, Lapouyade R (1989) Non-radiative deactivation channels of molecular rotors. J PhotochemPhotobiolA 48(1):87–93
13. Förster T, Hoffmann G (1971) Die Viskositätsabhängigkeit der Fluoreszenzquantenausbeuten einiger Farbstoffsysteme [The viscosity dependency of the fluorescent quantum yield of some dye systems]. Zeitschrift für Physikalische Chemie 75:63–76
14. Howell S, Dakanali M, Theodorakis EA, Haidekker MA (2012) Intrinsic and extrinsic temperature-dependency of viscosity-sensitive fluorescent molecular rotors. J Fluoresc 22(1):457–465
15. Haidekker MA, Nipper M, Mustafic A, Lichlyter D, Dakanali M, Theodorakis EA (2010) Dyes with segmental mobility: molecular rotors. In: Demchenko A (ed) Advanced fluorescence reporters in chemistry and biology I. Springer, Berlin Heidelberg New York, pp 267–308
16. Kung CE, Reed JK (1989) Fluorescent molecular rotors: a new class of probes for tubulin structure and assembly. Biochemistry 28(16):6678–6686
17. Sawada S, Iio T, Hayashi Y, Takahashi S (1992) Fluorescent rotors and their applications to the study of GF transformation of Actin. Anal Biochem 204(1):110–117
18. Kuimova MK, Botchway SW, Parker AW, Balaz M, Collins HA, Anderson HL et al (2009) Imaging intracellular viscosity of a single cell during photoinduced cell death. Nat Chem 1(1):69–73
19. Haidekker MA, Akers W, Lichlyter D, Brady TP, Theodorakis EA (2005) Sensing of flow and shear stress using fluorescent molecular rotors. Sens Lett 3(1):42–48
20. Mustafic A, Huang HM, Theodorakis EA, Haidekker MA (2010) Imaging of flow patterns with fluorescent molecular rotors. J Fluoresc 20(5):1087–1098
21. Rumble C, Rich K, He G, Maroncelli M (2012) CCVJ is not a simple rotor probe. J Phys Chem A 116(44):10786–10792
22. Sutharsan J, Dakanali M, Capule CC, Haidekker MA, Yang J, Theodorakis EA (2010) Rational design of amyloid binding agents based on the molecular rotor motif. ChemMedChem 5(1):56–60
23. Haynes WM (2011) CRC handbook of chemistry and physics. CRC Press, Boca Raton